Eur. Phys. J. D **22**, 3–11 (2003)
DOI: 10.1140/epjd/e2002-00213-1

THE EUROPEAN PHYSICAL JOURNAL D

Two-color pump-probe experiments in helium using high-order harmonics

A. Johansson[1], M.K. Raarup[2,a], Z.S. Li[1], V. Lokhnygin[1,b], D. Descamps[1,c], C. Lyngå[1,d], E. Mevel[1,e], J. Larsson[1], C.-G. Wahlström[1], S. Aloise[3], M. Gisselbrecht[3,f], M. Meyer[3], and A. L'Huillier[1,g]

[1] Department of Physics, Lund Institute of Technology, P.O. Box 118, 221 00 Lund, Sweden
[2] Institute of Physics and Astronomy, University of Aarhus, 8000 Aarhus C, Denmark
[3] LURE, Centre Universitaire Paris-Sud, Bâtiment 209D, 91898 Orsay Cedex, France
and
CEA/DRECAM/SPAM, CEN Saclay, 91105 Gif-sur-Yvette, France

Received 3 June 2002 / Received in final form 14 August 2002
Published online 22 October 2002

Abstract. A pump-probe technique has been applied for measuring the lifetimes and absolute photoionization cross-sections of excited He states. The $1s2p\ ^1$P and $1s3p\ ^1$P states of He are excited by using the 13th and the 14th harmonic, respectively, of a tunable 70 ps dye laser generated in a Kr gas jet. The states are ionized after a varying time delay, by absorption of probe photons with energies between 1.6 and 4.5 eV. Lifetimes of $\tau(1s2p) = 0.57$ ns and $\tau(1s3p) = 1.76$ ns are determined with a precision of about 15%. A significant enhancement of the number of ions present in the lifetime curves at zero time delay for pressures above 6×10^{-5} mbar is attributed to direct two-photon ionization of He in combination with AC Stark broadening of the excited state and absorption of the XUV light in the medium. Absolute photoionization cross-sections from the He $1s2p\ ^1$P and He $1s3p\ ^1$P states in the threshold region are determined by measuring the saturation of the ionization process with a precision of $\sim 25\%$. In addition, the variation of the relative orientation between the polarization vectors of the pump and probe beams enables the determination of partial photoionization cross-sections.

PACS. 32.70.Cs Oscillator strengths, lifetimes, transition moments – 32.80.Fb Photoionization of atoms and ions – 42.65.Ky Harmonic generation, frequency conversion

1 Introduction

Two-photon pump-probe experiments combining an XUV and an UV/visible photon source have shown to be ideally suited for studying the excitation and relaxation of excited states in atoms and molecules. In particular, the application of short pulse light sources offers the possibility to follow the temporal evolution of the excited states, which decay by radiative or nonradiative transitions with lifetimes ranging from the femtosecond to the nanosecond range. As an example, the two-photon excitation scheme of atomic He is presented in Figure 1. Here the XUV photon is used to prepare in a controlled and well-defined way a specific excited state. The time-dependent population decay of this state is then probed by a second time-delayed photon inducing photoionization.

Experiments combining synchrotron radiation and conventional continuous-wave lasers have mainly concentrated on laser-excited atoms where the outer electron is manipulated by the laser light (*e.g.* [1,2]). Only a few studies have been undertaken to extend these type of experiments to time-resolved measurements by synchronizing a pulsed, mode-locked, laser to the MHz repetition rate of the synchrotron radiation pulses [3,4]. The dynamical range of these studies is mainly determined by the temporal widths of the synchrotron pulses (from 500 ps to 30 ps for second and third generation synchrotron radiation sources, respectively) and the interpulse distance (up to some hundreds nanoseconds). The recent developments in the generation of high-order harmonics in rare gases by an intense, pulsed laser have established this radiation as an alternative excitation source. Although in general limited in tunability and energy range with respect

[a] *Present address*: Department of Biophysics, Leiden University, 2333 CA Leiden, The Netherlands.
[b] *Present address*: Continuum Electro-Optics Inc., 3150 Central Expressway, Santa Clara, CA 95051, USA.
[c] *Present address*: CEA/DRECAM/SPAM, CEN Saclay, 91105 Gif-sur-Yvette, France.
[d] *Present address*: Department of Physics, National University of Rwanda, Butare, Rwanda.
[e] *Present address*: CELIA, Université Bordeaux 1, 33405 Talence, France.
[f] *Present address*: MAX-Lab, Lund University, Box 118, 221 00 Lund, Sweden.
[g] e-mail: `anne.lhuillier@fysik.lth.se`

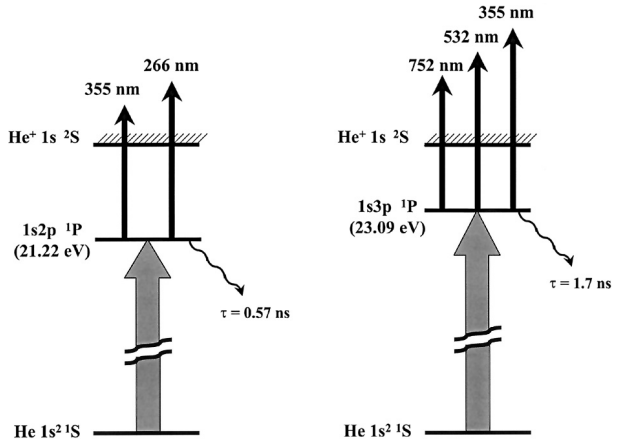

Fig. 1. Energy level diagram of He indicating the atomic states and the two-color ionization schemes involved in the lifetime and photoionization cross-section measurements.

to synchrotron radiation, the high-order harmonics offer the advantages of being of short pulse duration (in the picosecond or femtosecond range) [5], as well as being naturally synchronized to laser pulses. Pump-probe experiments using high harmonics can therefore be considered as pioneer studies and showcases for experiments, which are presently planed and discussed in connection with the new, linear accelerator based short-wavelength Free-Electron-Lasers [6].

From a scientific point of view, the results of a pump-probe study where a state is prepared by absorption of the pump pulse and ionized by absorption of a probe pulse, provide knowledge about (radiative or nonradiative) lifetimes as well as excitation- and ionization cross-sections. This knowledge is essential for many fundamental investigations, for example the characterization of plasmas [7], the interpretation of astrophysical spectra, the modelling of stellar properties [8] and the understanding of photochemical processes in the atmosphere [9].

Radiative lifetimes can be measured by a variety of methods [11]. For measurements of short (subnanosecond) lifetimes of states lying in the VUV/XUV region of the spectrum, the most appealing method is the pump-probe technique using a short harmonic pulse for the excitation and a short laser pulse for the detection. To demonstrate the capability of this technique, Larsson *et al.* [12] have determined the 0.57 ns lifetime of the He $1s2p$ ^{1}P state with an accuracy of 5%. The technique has also been applied to lifetime measurements of excited states of CO [13] and N_2 [14]. A similar setup, using pump/probe pulses in the 100 fs range and photoelectron spectroscopy to monitor the decay has been used to study dissociation of Rydberg states in acetylene [15].

Gisselbrecht *et al.* [16] have shown that pump-probe excitation schemes can also be used to determine absolute photoionization cross-sections for excited states by varying the pulse energy of the probe at a fixed time delay. Absolute values for the photoionization cross-section in the near-threshold region have been obtained for the $1s2p$ ^{1}P and $1s3p$ ^{1}P states of He for three different photon energies of the probe. These results represent the first systematic investigation of the energy dependent photoionization cross-section of excited He states and are found to be in good agreement with theory [17,18]. Other recent absolute excited-state photoionization cross-section measurements have concentrated on the heavier noble gas elements [19].

The present paper is a follow-up and extension of the studies in helium presented in [12,16]. We present in detail the pump-probe technique used for measuring the lifetime of excited states of He and for the determination of their absolute photoionization cross-sections. The main objective is to demonstrate the originality of the technique and to discuss some specific results obtained in the pump-probe experiments on atomic He. Furthermore, we have investigated an experimental peculiarity induced by direct two-photon ionization of He in combination with a significant absorption of the XUV light in the medium. It leads to a strong increase in the number of ions at zero time delay between the pump- and the probe-pulses and can severely affect the determination of short lifetimes. Finally, an extension of the method is presented showing that also partial (absolute) photoionization cross-sections can easily be determined by making use of the well-defined polarization characteristics of the high harmonics.

2 Experimental approach

2.1 Laser system

A schematic presentation of the experimental setup, common to the lifetime- and photoionization cross-section measurements, is shown in Figure 2. The tunable laser pulses needed for the resonant excitation of the $1s2p$ ^{1}P and $1s3p$ ^{1}P levels of He are generated by a distributed feedback dye laser (DFDL) similar to that described earlier [20,21]. The oscillator consists of a dye cell in which a dynamic (Bragg) grating, *i.e.* a periodic variation of the inverse population and refractive index, is created by two interfering pump beams. A Nd:YAG pump laser beam (532 nm, 10 Hz, 70 ps) is focused into the dye cell by a cylindrical lens after being diffracted from a 1200 lines/mm holographic plane grating. The beams diffracted in the +1 and −1 orders are recombined in the dye cell by two mirrors and a prism (see Fig. 2), providing the feedback for radiation at a wavelength equal to half the period of the induced grating. The DFDL wavelength is given by $\lambda_{\mathrm{dye}} = \lambda_{\mathrm{p}} n_{\mathrm{s}} / \sin\theta_{\mathrm{L}}$, where λ_{p} is the pump wavelength, n_{s} the refractive index of the dye solution and θ_{L} the angle between the incident laser beams and the normal to the surface of the dye cell. The wavelength of the radiation can be tuned by turning the mirrors, thus altering θ_{L}, or, on a finer scale, by changing the temperature of the dye cell, thus modifying the refractive index.

The advantage of an oscillator with distributed feedback consists in the production of close to Fourier-transform limited picosecond laser pulses, which can easily be tuned in wavelength [20,21]. In the experiments presented here, the pulse duration of the DFDL is about 70 ps. The absolute wavelength (in the near infrared region

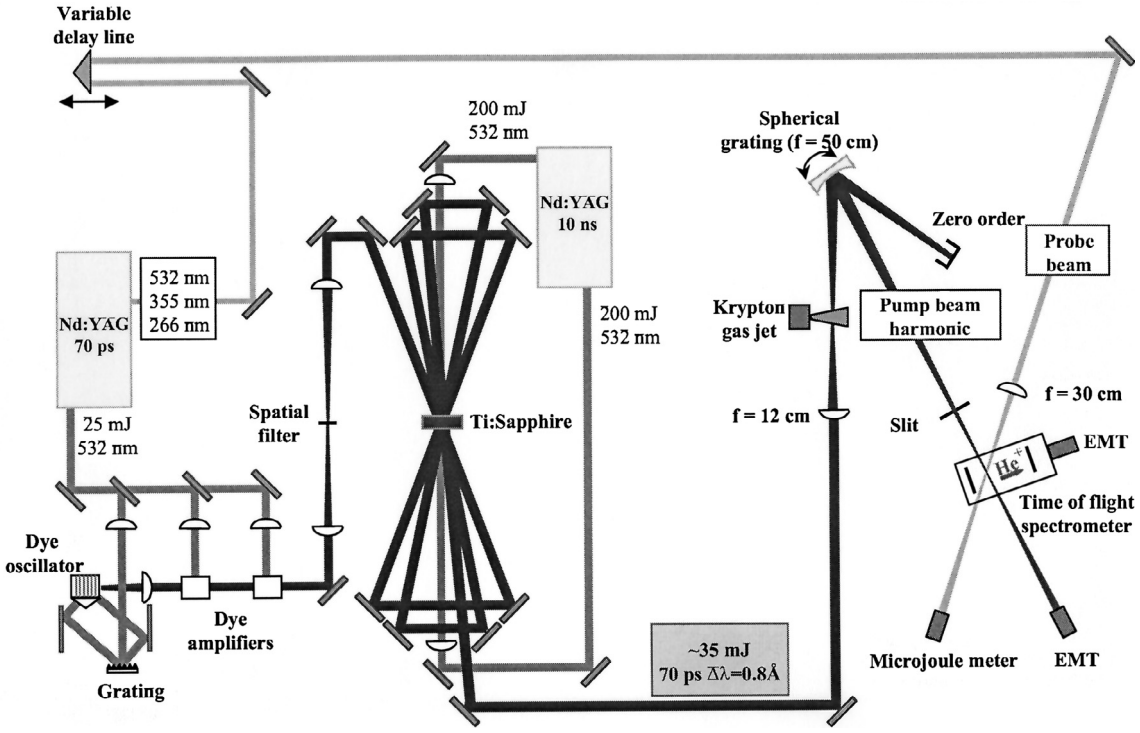

Fig. 2. A schematic presentation of the experimental set-up. A detailed description is given in the text.

around 750 nm) is measured with a wavemeter (Burleigh) to an accuracy of about 0.01 nm. The output from the DFDL oscillator is amplified to ∼1.5 mJ/pulse through two dye cell amplifiers pumped by the 70 ps Nd:YAG pump laser. Further amplification of the DFDL output to ∼35 mJ/pulse is obtained by five passages through a Ti:sapphire butterfly amplifier pumped with 400 mJ pulses from a second Nd:YAG laser (532 nm, 10 Hz, 10 ns).

2.2 Probe beam

Part of the output of the picosecond Nd:YAG laser is used to generate probe pulses at different photon energies through wave-mixing processes. The wavelengths used in the cross-section measurements are indicated in Figure 1. For the lifetime measurements of the He $1s2p$ ^{1}P and $1s3p$ ^{1}P states, probe wavelengths of 355 nm and 532 nm, respectively, are used. The probe beam passes through a delay line on its way to the interaction region (see Fig. 2) allowing for variation and control of the time-delay between pump and probe pulses. A halfwave plate enables the rotation of the polarization vector of the linearly polarized laser light with respect to that of the harmonic beam.

In the cross-section measurements, the probe energy, measured with a power meter, is varied from a few to a few hundreds μJ. The uncertainty in the energy determination is estimated to ±15%. In the lifetime measurements, the probe energy is set to a value around the saturation of the ionization process (∼ 100 μJ, *i.e.* some 10^{14} photons per pulse). This implies that approximately all the atoms excited in the interaction region (about 10 to 1000) are ionized by the probe beam. The probe pulse duration is measured by a streak camera to be about 70 ps.

The probe beam intersects the harmonic (pump) beam at a 45° angle in the interaction volume of the vacuum chamber. It is focused with a $f = 30$ cm lens a few cm in front of the interaction region. The determination of the photoionization cross-section in absolute value, based on the saturation of the ionization step [22] (see below), requires the characterization of the spatial profiles of the probe (and pump) beam in the interaction region. A beam splitter is therefore placed between the lens and the vacuum chamber and a small fraction of the probe beam is sent onto a CCD camera chip installed at the same distance from the beam splitter as the interaction region. A diameter of about 100 μm is determined for the probe beam in the interaction region, corresponding to an intensity of 5×10^8 W/cm^2. This intensity is too low to induce any significant multiphoton ionization.

2.3 Pump beam

For excitation of the He $1s2p$ ^{1}P state at an energy of 21.22 eV, the DFDL is tuned to the wavelength $\lambda_{\rm dye} =$ 759 nm. The beam is focused into a Kr gas jet with a lens of 12 cm focal length. The intensity is about $\sim 5 \times 10^{14}$ W/cm^2 at the beam waist. High-order harmonics are emitted on axis, separated by a normal incidence 1200 lines/mm spherical grating and detected by an electron multiplier tube (see Fig. 2). A typical spectrum is presented in Figure 3a showing odd harmonics up to the 21st order. By tuning the DFDL wavelength which causes also a variation in the photon energy of the harmonics,

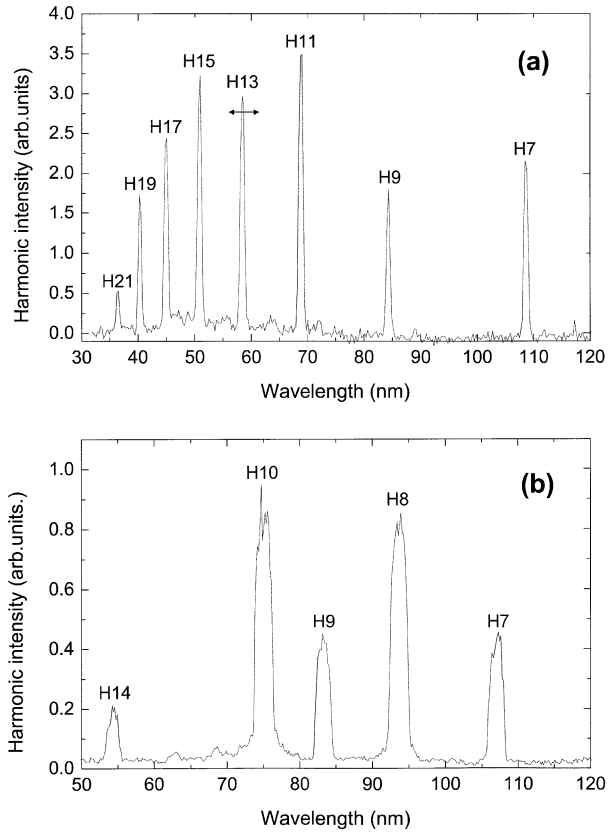

Fig. 3. Typical spectrum of high-order harmonics generated with (a) the fundamental wavelength of the DFDL and (b) the fundamental and the second harmonic. The range of tunability obtained for the 13th harmonic using the dye LDS751 is indicated.

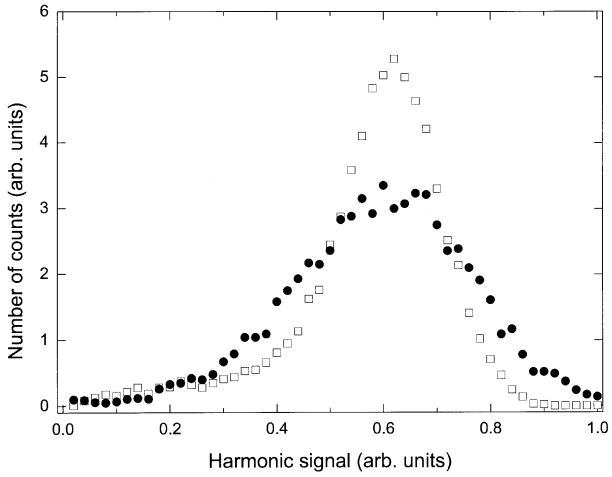

Fig. 4. Distribution of the 13th (open squares) and 14th (filled circles) harmonic signals for a given pump energy.

and by selecting different harmonics with the grating, a quasi-tunable XUV source is available for the experiments. The tunability range for the 13th harmonic, which is selected to excite the He $1s2p$ ^{1}P state, is indicated by an arrow in the figure.

A slightly different approach is used to excite the He $1s3p$ ^{1}P resonance at 23.09 eV. The laser is tuned to a wavelength $\lambda_{\rm dye} = 753$ nm and frequency doubled in a type II KDP crystal. Both the fundamental and the second-harmonic pulses are focused into the Kr gas jet. The beam walk off in the doubling crystal is negligible for the picosecond pulses used in these experiments. The resulting spectrum (Fig. 3b) contains therefore both even and odd harmonics of the fundamental frequency, which result from different wave-mixing processes. This technique allows us to increase the tunablity range. The 14th harmonic is selected to excite the He $1s3p$ ^{1}P state.

A 2 mm wide slit is used to select the desired harmonic without intercepting it, blocking the fundamental beam and all the other harmonic orders. The number of 13th (or 14th) harmonic photons present in the interaction chamber is determined with a calibrated XUV-sensitive diode placed after an aluminum filter to about 5×10^6 per pulse. The transmission of the grating is at best 10%, meaning that at least 5×10^7 photons are generated at each laser shot.

Due to the non-linear process for the production of high-order harmonics the harmonic photon flux exhibits a significant shot-to-shot variation. Figure 4 shows the relative fluctuations for the 13th and 14th harmonics. The distributions can be characterized by a Gaussian profile with a full width at half maximum of about 20–30% of the mean value. For the 14th harmonic a slightly larger variation is observed, indicating more fluctuations in the region close to the cut-off of the harmonic generation spectrum (see Fig. 3b). In most experiments, it is therefore necessary to integrate over a sufficiently large number of pulses in order to compensate for these intensity fluctuations. Typical integration times vary from one to twenty minutes for each data point. Alternatively, it is possible to monitor at 10 Hz repetition rate the intensity of the pump and probe beam as well as the ion signal for each individual pulse. In this way a "shot-rejection" filter can be introduced allowing us to select only those events, which are produced in a well-defined intensity range of the excitation sources.

In order to determine the spatial profile of the pump beam, the number of ions produced (for a given probe) are recorded as a function of the vertical position of the lens used to focus the probe beam. The curve obtained is proportional to the convolution of the probe and the pump spatial profiles. The harmonic beam diameter is estimated to about 500 μm in the interaction region. The pulse duration of the 13th harmonic is measured with an XUV streak camera to be $\sim$30 ps.

The bandwidth of the harmonics is determined by measuring the He^+ signal, which is induced by the two-step excitation, as a function of the DFDL wavelength in the region around the He $1s2p$ ^{1}P resonance. The resulting spectrum recorded at a fixed pump-probe delay (taken at a delay of 230 ps) for the 13th harmonic is presented in Figure 5. The solid line is a Gaussian fit to the experimental data points, from which a full width at half maximum of 3.5 pm (1.3 meV) is deduced. Due to the

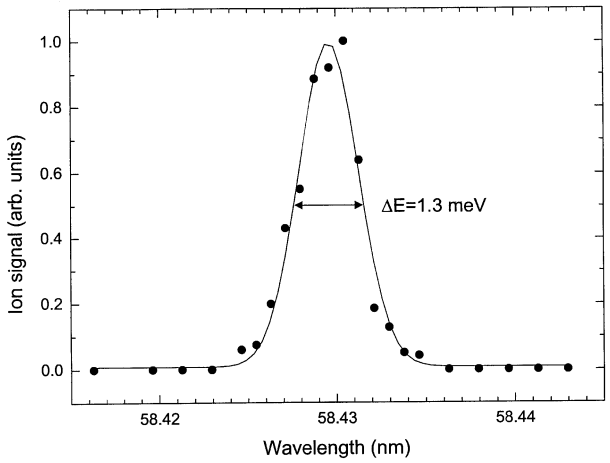

Fig. 5. Excitation spectrum of the He $1s2p$ ^{1}P state. The total number of ions produced by the two-photon excitation is recorded as a function of the photon energy of the pump beam. The spectrum shows essentially the spectral profile of the 13th harmonic.

Doppler-broadened width of 0.13 meV for the He $1s2p$ ^{1}P level, this value represents essentially the spectral width of the harmonics.

2.4 Ion detection

The interaction region defined by the intersection of an effusive He gas jet and the photon beams is surrounded by two grids separated by about 2 cm. The ions produced are extracted from this region by applying a 1 kV potential difference and accelerated towards a 70 cm-long field-free flight tube, which is terminated with an electron multiplier tube (EMT). The He^+ ions are selected with respect to their time of flight by using the signal from the harmonic pulses as a start trigger. No He^+ ions are detected when only one of the photon beams is present in the experimental chamber. The background pressure in the experimental chamber is below 1×10^{-6} mbar without the gas jet. The He gas is introduced through a 500 μm orifice which can be operated in a pulsed mode, but is usually used with a continuous flow. During the experiments the background pressure is increased to values between some 10^{-6} and 1×10^{-4} mbar.

3 Lifetime measurements

In a first type of application, the described set-up is used to determine the lifetimes of excited states by changing in a controlled way the temporal delay between the pump (XUV) and the probe (UV-visible) pulse. Typical decay curves of the He $1s2p$ ^{1}P and $1s3p$ ^{1}P states are displayed in Figures 6a and 6b, respectively, showing on a logarithmic scale the number of He^+ ions as a function of the delay time. The photon energy of the probe laser is chosen to ionize the excited $1snp$ ^{1}P states in the region close to threshold, thus optimizing the ionization cross-section and preventing the ionization of lower-lying He $1sns$ ^{1}S

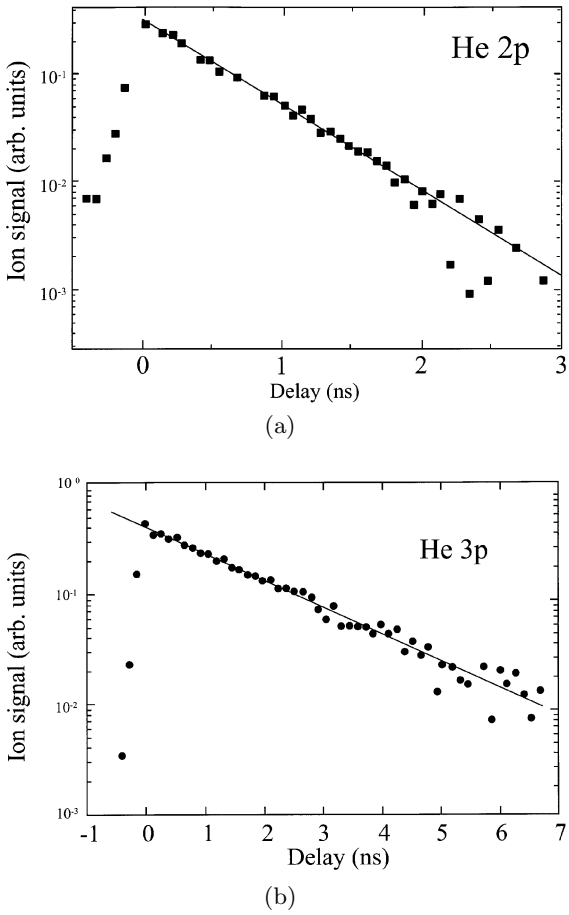

Fig. 6. He^+ ion signal as a function of the temporal delay between the pump and the probe pulse. (a) Decay curve recorded upon excitation of the He $1s2p$ ^{1}P state at a static pressure of 7×10^{-6} mbar; (b) upon excitation of the He $1s3p$ ^{1}P state at 2×10^{-5} mbar.

states, which can be populated by radiative relaxation. For the He $1s2p$ ^{1}P resonance, we use a probe energy of 3.5 eV (355 nm). For the He $1s3p$ ^{1}P resonance, the probe photon energy (2.2 eV, 532 nm) is high enough to ionize also those atoms which have relaxed to the He $1s3s$ ^{1}S state lying only 0.16 eV below the $1s3p$ ^{1}P state. However, the influence on the measurements is estimated to be very small, because the radiative transition to the He $1s^2$ ^{1}S ground state is by far the dominant process. Only less than 0.1% of the $1s3p$ ^{1}P excited states are estimated to decay to the $1s3s$ ^{1}S level.

The decay curves (Fig. 6) show clearly that the logarithm of the signal varies linearly with the delay time over more than 4 lifetimes (2 ns) allowing us to determine the lifetime with good accuracy. The measurements yield lifetimes of 0.57 ± 0.03 ns for the $1s2p$ state and 1.76 ± 0.1 ns for the $1s3p$ state, in good agreement with previous data having about the same level of precision [23].

In some conditions, we find that the exponential decay characteristic of lifetimes measurements can be perturbed by a significant enhancement of the number of ions at very

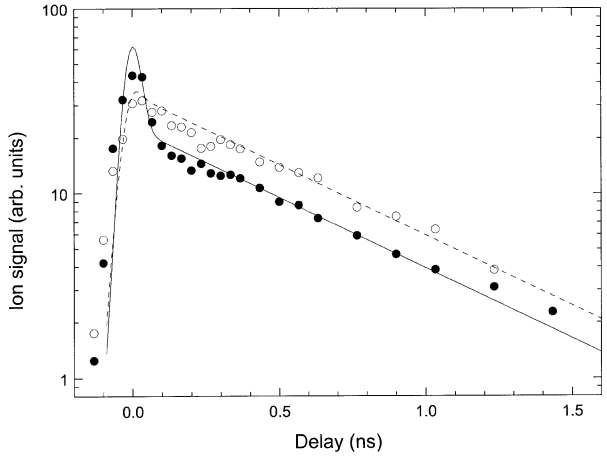

Fig. 7. He^+ ion signal as a function of pump-probe delay at a static pressure of 6×10^{-5} mbar (open circles) and 1×10^{-4} mbar (solid circles). The laser is tuned to excite the $1s2p$ state. The dashed and solid lines are theoretical predictions obtained at static pressures of 2.5×10^{-8} mbar and 1×10^{-7} mbar respectively.

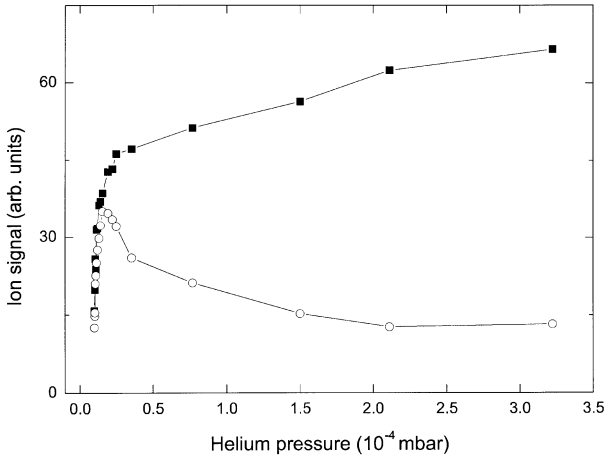

Fig. 8. He^+ ion signal as a function of pressure at zero time delay (squares) and at a time delay of 230 ps (circles).

short time delays. Since this enhancement requires that the pump and probe beams overlap in time, we attribute it to a "direct" two-photon ionization process. Two measurements for the He $1s2p$ excited state, are presented in Figure 7. When increasing the He gas pressure from 6×10^{-5} mbar (open circles) to 1×10^{-4} mbar (solid circles) the general form of the decay curves changes drastically. At long time delays (> 200 ps) both curves show the same exponential decrease indicating that the lifetime of the intermediate state is not affected by the increase of pressure. On the other hand the signal obtained at high pressures is reduced for time delays longer than 200 ps and shows a significant increase ("spike") around zero pump-probe delay. This effect can strongly affect the determination of short lifetimes, comparable to the temporal width of the photon pulses.

In order to gain more insight in the underlying mechanism for the spike, the ion signal has been measured as a function of the gas pressure at two different time delays: 0 ps ("on-spike", filled squares) and 230 ps ("off-spike", open circles), as shown in Figure 8. At low He densities ($\leq 3 \times 10^{-5}$ mbar) both signals increase linearly with the gas pressure. For pressures higher than 5×10^{-5} mbar the "off-spike" signal is strongly reduced indicating the influence of absorption of the exciting XUV pump pulse. This absorption is caused by the propagation of the harmonic beam through a rather long pathway in the vacuum chamber containing a non-negligible quantity of He gas. In contrast, the "on-spike" signal increases up to $\sim 6 \times 10^{-4}$ mbar and then saturates. An additional mechanism compensates the loss in efficiency for the pump process.

The results shown in Figures 7 and 8 can be understood by a combination of absorption of the XUV photons in the He gas and AC-Stark broadening of the $1s2p$ state at zero time delay, when both pulses are present in the interaction volume. Only the spectral region corresponding to the Doppler-broadened profile is affected by absorption outside the interaction region, and a "hole" is burned in the harmonic profile (the harmonic width is much broader than the Doppler width, as discussed in Sect. 2.3). This leads, in general, to a reduced efficiency in the ionization process. When the pump and probe pulses overlap in time, however, the Stark-broadening of the absorption profile allows also excitation by photons of slightly different photon energy. As a consequence, the ion signal is enhanced and the decay curves exhibit a "spike" as a function of time delay. The conditions necessary for the observation of the "spike" are thus: (i) a probe intensity sufficiently high to induce a significant broadening of the $1s2p$ level and (ii) a significant absorption of the XUV pulse by He gas before reaching the overlap region.

The observations can be approximately accounted for by a rate-equation model [24–26] based on the following equations:

$$\frac{\mathrm{d}N_\mathrm{g}}{\mathrm{d}t} = -\Omega(t)N_\mathrm{g}, \tag{1}$$

$$\frac{\mathrm{d}N_\mathrm{r}}{\mathrm{d}t} = \Omega(t)N_\mathrm{g} - \Gamma_\mathrm{r}^\mathrm{UV}(t)N_\mathrm{r} - A_\mathrm{r}N_\mathrm{r}, \tag{2}$$

$$\frac{\mathrm{d}N_\mathrm{i}}{\mathrm{d}t} = \Gamma_\mathrm{r}^\mathrm{UV}(t)N_\mathrm{r} \tag{3}$$

$N_\mathrm{g}(t)$, $N_\mathrm{r}(t)$ and $N_\mathrm{i}(t)$ represent the ground state, resonant excited state and ion populations. $\Gamma_\mathrm{r}^\mathrm{UV}(t)$ is the ionization probability of the resonant level due to the probe beam, which depends on the delay between probe and pump pulses, A_r the inverse of the radiative lifetime, and $\Omega(t)$ the rate for excitation from the ground to the excited state. We here assume a small population transfer to the exited state, so that stimulated emission back to the ground state can be neglected. Using the measured ionization cross-section from the $1s2p$ state with a photon energy of 3.5 eV (355 nm) $\sigma = 16.6$ Mbarn (see [16] and Sect. 4), we have $\Gamma_\mathrm{r}^\mathrm{UV}(0) = 13\ \mathrm{ns}^{-1}$ at zero time delay, for a probe intensity $I = 5 \times 10^8$ W/cm^2. This implies that

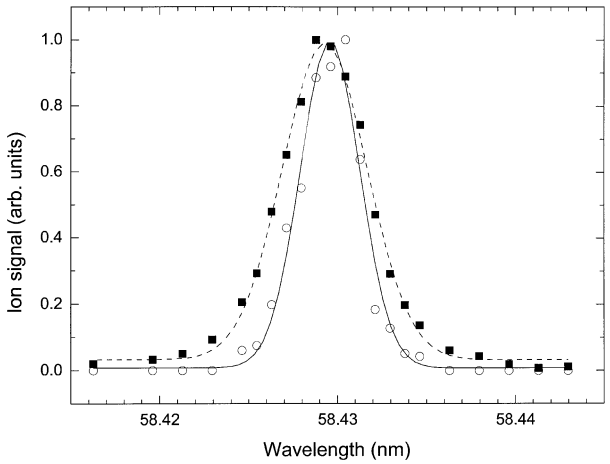

Fig. 9. Excitation spectrum of the He $1s2p$ ^{1}P state. In open circles, the time delay is set to 230 ps. The spectrum shown in full squares is obtained at zero time delay and exhibits a broadening and a shift to the AC Stark effect.

the transition is almost saturated ($\Gamma_{\rm r}^{\rm UV}(0) \times \tau^{\rm UV} = 0.9$, where $\tau^{\rm UV}$ is the pulse duration of the UV probe pulse). As pointed out above, absorption in He gas reduces the number of XUV photons available for excitation. However, the number of useful photons, and therefore the excitation rate $\Omega(t)$ is less reduced when pump and probe overlap in time, since the absorption profile is broadened in presence of the probe pulse. We take this effect into account in a phenomenological way by multiplying for each pump-probe delay the (Stark-broadened) Lorentzian profile with the exponential absorption factor of the Beer-Lambert's law, using the wavelength-dependent field-free Lorentzian absorption cross-section in the exponent. The excitation rate $\Omega(t)$ is proportional to the integral of the Stark-broadened "hole-burned" transition profile, and thus depends on the time delay between probe and pump pulses. equations (1–3) can then be solved numerically to yield the ion signal $N_{\rm i}(t)$.

Results obtained for pressures of 2.5×10^{-8} and 1×10^{-7} mbar are shown as the dashed and solid lines in Figure 7, respectively. The overall agreement between experimental data points and the simulations is quite reasonable, although the development of the "spike" is predicted by the rate-equation model to occur at somewhat lower pressure than found experimentally. This indicates that absorption should be treated in a more correct fashion, requiring the combined solution of Schrödinger's and Maxwell's equations. Our model, however, is capable of predicting the essential features of the observations. The influence of radiation trapping and pressure broadening [10,27] can be considered insignificant in the present experiment due to the low harmonic photon flux and given the pressure-independent slopes of the decay curves in Figure 7.

The influence of the Stark-broadening can also be observed by measuring directly the He $1s2p$ ^{1}P resonance profile using a fixed photon energy of the probe (Fig. 9). When the temporal delay is chosen to be 230 ps (open circles), the resonance profile reflects the spectral width of the harmonics and allows us to characterize the harmonic radiation source (*cf.* Sect. 2.3). When the two beams overlap in time (filled squares), the spectral profile is substantially broadened and slightly shifted to higher energies. The probe intensity used for this measurement is estimated to 5×10^8 W/cm^2. A fit to the experimental data with a Gaussian profile (dashed line) gives a FWHM (full width at half maximum) of 5.7 pm (2.0 meV) and a shift towards shorter wavelengths of 0.3 pm (0.11 meV). The ionization width can be calculated to be 5.6 pm, in very good agreement with the experimental observations. The experimental shift of 0.3 pm is higher than that measured at higher probe wavelength (292 nm) by Eikema and coworkers [28], equal to 0.015 pm for our probe intensity.

Although the investigated effect is rather an artefact to avoid in lifetime measurements, it opens the way to new phenomena, which can be studied in a (1+1)-photon setup, like cross-correlation measurements or coupling between autoionization states. With the advent of new sources delivering intense and ultrashort VUV pulses together with synchronized IR/visible pulses detailed insights into the coupling and interactions between electrons and photons can be obtained. In particular, these experiments will allow one to obtain complementary information on the dynamics of the fast Auger decay as well as of the electronic correlations in the ionization continua.

4 Photoionization cross-section measurements

For measurements of the photoionization cross-section of the excited He $1s2p$ and $1s3p$ states [16], the pump-probe delay is set to 230 ps in order to completely separate the excitation and ionization steps, thus avoiding processes arising from the temporal overlap of both excitation pulses (*cf.* Sect. 3). Pump and probe pulses are sufficiently short that the spontaneous decay of the excited states during the excitation and ionization processes can be neglected. The photoionization cross-section can be determined by recording the number of He^+ ions, for fixed photon energies of the pump and the probe beams, as a function of energy in the probe beam, *i.e.* the number of probe photons. A typical experimental result obtained for He $1s2p$ with a probe wavelength of 355 nm is presented in Figure 10. The ion signal varies first linearly with the probe energy (see dashed line), and then saturates, because the ionization probability in the interaction region is close to one. The number of ions produced is proportional to [16]

$$N_{\rm i} \propto \int R_{\rm pump} \left(1 - \exp\left(-\sigma_{\rm ion} R_{\rm probe}\right)\right) {\rm d}V, \qquad (4)$$

where $R_{\rm probe}$ ($R_{\rm pump}$) is the space-dependent number of probe (pump) photons per unit area and $\sigma_{\rm ion}$ the ionization cross-section, which depends on the polarization of the probe relative to the pump. For a given pump energy, the saturation of the ion signal depends only on the product $\sigma_{\rm ion} R_{\rm probe}$. Knowing the spatial profiles of both the

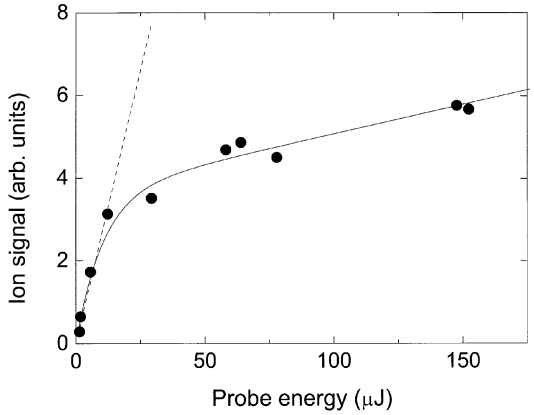

Fig. 10. He^+ ion signal as a function of the energy of the probe pulse. He atoms are prepared in the He $1s2p$ excited state and the probe laser is set to a wavelength of 355 nm. The dashed line indicates the linear, unsaturated regime. The solid line represents a fit to the experimental data using a three-dimensional integration as discussed in the text.

Table 1. Absolute photoionization cross-sections for the $1s2p$ ^{1}P and $1s3p$ ^{1}P state for different probe wavelengths (excitation energies). We also indicate the corresponding excess energy (energy above threshold) $E_{\rm exc}$. The experimental values are obtained using a parallel orientation between the polarization vectors of the pump and the probe beams.

Excited state	$\lambda_{\rm probe}$(nm)	$E_{\rm exc}$(eV)	$\sigma_\parallel$(Mb)
$1s2p$ ^{1}P	355	0.12	16.6
	266	1.29	6.6
$1s3p$ ^{1}P	752	0.15	24.4
	532	0.83	10.5
	355	1.99	4.2

pump and the probe beams, as well as the energy in the probe beam, the absolute value of the ionization cross-section is determined by fitting the experimental data to the three-dimensional integral in equation (4), using $\sigma_{\rm ion}$ as a free parameter. Due to volume effects, the number of ions continues to increase as a function of the probe energy, even far into the saturation regime (see Fig. 10).

The experimental results for the determination of the absolute cross-section of the excited He $1s2p$ and $1s3p$ states, using a parallel orientation between the polarization vectors of the pump and the probe beam, are summarized in Table 1. The extracted numbers illustrate the strong dependence of the photoionization cross-section for the excited He $1snp$ states in the region close to the ionization threshold. In addition, the photoionization cross-section is larger for $n = 3$ than for $n = 2$ at the same excess energy $E_{\rm exc}$ (*i.e.* energy above threshold). The total uncertainty for the absolute values is estimated to about 25% and the experimental results confirm the available theoretical data [17,18] as described in more details in [16].

In addition, the well-defined linear polarization of the pump and probe pulses has been exploited. By varying the relative orientation between the two polarization vectors it is possible to extract the isotropic partial ionization cross-sections, *i.e.* the polarization-independent cross-sections for ionization into the ϵs and ϵd continuum. Ionization from the excited He $1snp$ ^{1}P$_1$ states leads to a He^+ ion in the $1s$ ^{2}S$_{1/2}$ ground state. Due to conservation of angular momentum, one-photon ionization of the $1snp$ ^{1}P$_1$ state results in the emission of either an s- or d-wave electron, corresponding to a total final-state momentum of ^{1}S$_0$ or ^{1}D$_2$, respectively:

$$\begin{aligned} {\rm He}^*1snp\ ^1{\rm P}_1 + h\nu &\longrightarrow ({\rm He}^+1s\ ^1{\rm S}_{1/2} + \varepsilon_s)\ ^1{\rm S}_0 \\ &\longrightarrow ({\rm He}^+1s\ ^1{\rm S}_{1/2} + \varepsilon_d)\ ^1{\rm D}_2. \end{aligned}$$

The total photoionization cross-section, using linearly polarized photon beams, is given by [29]

$$\sigma(\theta_{\rm P}) = \sigma^{(\rm iso)} \left(1 - \sqrt{\frac{10}{3}}\,\beta_{202}\,\mathcal{A}_{20}(J_0)\,P_2(\cos\theta_{\rm P})\right), \quad (5)$$

where $\sigma^{(\rm iso)}$ is the photoionization cross-section for unpolarized light, $\mathcal{A}_{20}(J_0)$ describes the alignment of the $1snp$ ($J_0 = 1$) state, $P_2(\cos\theta_{\rm P}) = \frac{1}{2}(3\cos^2\theta_{\rm P} - 1)$ is the second-order Legendre polynomium, $\theta_{\rm P}$ the angle between the polarization vectors of the pump and the probe and the coefficient β_{202} is a particular case of the the dynamical coefficient β_{k_0kk}, containing the dipole amplitudes for the partial cross-sections. Within the LS-coupling scheme, the alignment and the dynamical coefficient can be expressed for the present example by $\mathcal{A}_{20}(J_0 = L_0) = -\sqrt{2}$ and

$$\beta_{202} = \frac{3}{\sigma^{(\rm iso)}}\sqrt{\frac{3}{5}}\sum_L \begin{Bmatrix} L_0 & L_0 & 2 \\ 1 & 1 & L \end{Bmatrix} \sigma(L_0 \to L). \quad (6)$$

$\sigma(L_0 \to L)$ represents the partial cross-sections for photoionization from the $1snp$ excited state with angular momentum L_0 to the final state, which is built up from the He^+ $1s$ ^{2}S ionic state and the outgoing s or d electron with total angular $L = 0$ and 2, respectively. The expression in brackets is the standard Wigner $6j$-symbol. In our case, the formula for the cross-section (Eq. (5)) reduces to

$$\sigma(\theta_{\rm P}) = \sigma_s + \sigma_d + 2\left(\sigma_s + \frac{1}{10}\sigma_d\right) P_2(\cos\theta_{\rm P}) \quad (7)$$

where σ_s and σ_d represent in a reduced notation the partial cross-sections for the emission of an s or d-electron, respectively.

For a given angle $\theta_{\rm P}$, and when the ionization process is far from saturation, the number of ions $N_{\rm i}$ is directly proportional to the total cross-section $\sigma(\theta_{\rm P})$. Thus, by measuring the number of ions as a function of angle and applying the above expression the ratio σ_d/σ_s can be determined. (In principle, it suffices to measure the ion signal for two different angles, *e.g.* $\sigma_\parallel = \sigma(\theta_{\rm P} = 0^\circ)$ and $\sigma_\perp = \sigma(\theta_{\rm P} = 90^\circ)$, corresponding to parallel- and perpendicular polarizations, respectively.) In Figure 11, the variation of the ion signal is given as a function of the angle $\theta_{\rm P}$. The fit to the experimental data points, indicated by the solid curve, yields a ratio of $\sigma_d/\sigma_s = 20/1$. This result

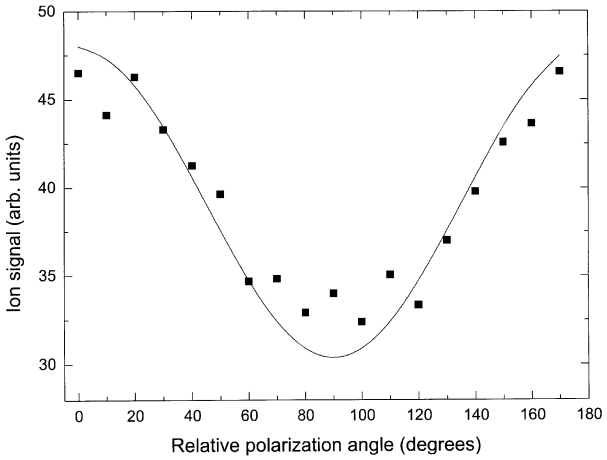

Fig. 11. He^+ ion signal as a function of angle between the polarization vectors of the pump and the probe beams. The theoretically predicted variation of the relative cross-section is indicated by the solid curve.

is in reasonable agreement with the theoretical ratio [17] $\sigma_d/\sigma_s = 13/1$, leading to a ratio $\sigma_\parallel/\sigma_\perp = 1.6$. The given example demonstrates the potential of this type of pump-probe experiments providing detailed information on the photoionization process by simply measuring the total ion signal. However, due to the large difference between the σ_d and σ_s cross-sections, the deduced ratio σ_d/σ_s is very sensitive to the amplitude of the cosine modulation and a more precise estimation is prevented due to the large scatter among the data points (statistical error of about 25%). This relatively poor statistics is caused by the experimental necessity to perform the experiment well below the saturation limit, *i.e.* with a reduced number of events.

5 Conclusion

The usefulness and potential of the two-color pump-probe technique using high-order harmonics for studies of lifetimes and photoionization cross-sections of excited states in the XUV has been demonstrated through measurements on He $1s2p\ ^1$P and $1s3p\ ^1$P levels. Lifetimes longer than 100 ps are determined with a precision of about 15%. A significant enhancement of the number of ions present in the lifetime curves at zero time delay for pressures above 6×10^{-5} mbar is attributed to a "direct" two-photon ionization process enhanced relative to (time-delayed) pump probe ionization, owing to a combination of resonant absorption of the XUV light and AC-Stark broadening of the excited level. Absolute photoionization cross-sections from the He $1s2p\ ^1$P and He $1s3p\ ^1$P excited states are determined in the threshold region with a precision of $\sim 25\%$. Finally, the relative polarization of the pump and probe beams can easily be varied, enabling the determination of partial photoionization cross-sections.

The two-color pump-probe technique using harmonics has only been used in a limited number of studies but can easily be applied for studies of many other systems. The advantages of this method are the inherent synchronization of the pump and the probe pulses, short pulse durations, a competitive bandwidth (at least in the photon energy range below 40 eV) and a table-top instrument.

This work was supported by the European Community *via* the TMR-grant "Access to Large Scale Facilities", contract ERBFMGECT950020(DG12). We acknowledge the support from the Swedish Science Research Council. M.R. acknowledges the support from Nordisk Forkerutdanningsakademi (NorFa). S.A., M.G. and M.M. thank the Lund Laser Center for support and hospitality. We thank E. Constant for valuable discussions concerning the origin of the "spike".

References

1. D. Cubaynes *et al.*, Phys. Rev. Lett. **77**, 2194 (1996)
2. Ph. Wernet *et al.*, Phys. Rev. A **64**, 042707 (2001)
3. M. Gisselbrecht, A. Marquette, M. Meyer, J. Phys. B **31**, L977 (1988)
4. M. Mitzutani *et al.*, J. Synchr. Rad. **5**, 1069 (1998)
5. P. Salières, A. L'Huillier, Ph. Antoine, M. Lewenstein, Adv. At. Mol. Opt. Phys. **41**, 83 (1999); T. Brabec, F. Krausz, Rev. Mod. Phys. **72**, 545 (2000); P. Salières, M. Lewenstein, Meas. Sci. Tech. **12**, 1818 (2001)
6. V. Ayvazyan *et al.*, Phys. Rev. Lett. **88**, 104802-1 (2002)
7. D. Attwood, *Soft X-rays and Extreme Ultraviolet Radiation, Principles and Applications* (Cambridge University Press, United Kingdom, 2000)
8. A. Dalgarno, S. Lepp, in *Atomic, Molecular and Optical Physics Handbook*, edited by G.W.F. Drake (AIP Press, New York, 1996)
9. B.J. Finlayson Pitts, J.N. Pitts Jr, *Atmospheric Chemsitry* (Wiley, New York, 1986)
10. S.J. Buckman, Rev. Mod. Phys. **66**, 539 (1994)
11. S. Svanberg, in *Atomic and Molecular Spectroscopy*, 3rd edn. (Springer-Verlag, 2001)
12. J. Larsson *et al.*, J. Phys. B **28**, L53 (1995)
13. P. Cacciani *et al.*, Astrophys. J. **499**, L223 (1998); Eur. Phys. J. D **15**, 47 (2001)
14. W. Ubachs *et al.*, Chem. Phys. **270**, 215 (2001)
15. S.L. Sorensen *et al.*, J. Chem. Phys. Lett. **112**, 8038 (2000)
16. M. Gisselbrecht *et al.*, Phys. Rev. Lett. **82**, 4607 (1999)
17. T.N. Chang, T.K. Fang, Phys. Rev. A **52**, 2052 (1995)
18. Z. Felfli, S. Manson, private communication
19. R. Kau *et al.*, Z. Phys. D **39**, 267 (1997)
20. W. Schade *et al.*, Appl. Opt. **29**, 3950 (1990)
21. C. Lyngå *et al.*, Appl. Phys. B **72**, 913 (2001)
22. V.N. Ischenko *et al.*, J. Sov. Laser Res. **2**, 120 (1981)
23. R.C.G. Ligtenberg *et al.*, Phys. Rev. A **49**, 2363 (1994)
24. Th. Freudenberg *et al.*, Z. Phys. D **36**, 349 (1996)
25. K. Johst, H. Johansen, Appl. Phys. B **48**, 479 (1989)
26. A. L'Huillier *et al.*, J. Opt. Soc. Am. B **6**, 1790 (1989)
27. A. Thorne *et al.*, in *Spectrophysics, Principles and Applications* (Springer, Berlin, 1999)
28. K.S.E. Eikema *et al.*, Phys. Rev. A **55**, 1866 (1997)
29. S. Baier *et al.*, J. Phys. B **27**, 3363 (1994)